Clinical Biomechanics 27 (2012) 218–225

Contents lists available at SciVerse ScienceDirect

Clinical Biomechanics

journal homepage: www.elsevier.com/locate/clinbiomech

Posterior motion preserving implants evaluated by means of intervertebral disc bulging and annular fiber strains

Frank Heuer [a], Hendrik Schmidt [a], Wolfram Käfer [b], Nicolas Graf [a], Hans-Joachim Wilke [a,*]

[a] Institute of Orthopaedic Research and Biomechanics, Director Prof. Lutz Claes, University of Ulm, Helmholtzstr. 14, 89081 Ulm, Germany
[b] Department of Orthopaedic Surgery, Chairman Prof. Dr. Heiko Reichel, University of Ulm, Oberer Eselsberg 45, 89081 Ulm, Germany

ARTICLE INFO

Article history:
Received 17 March 2011
Accepted 13 September 2011

Keywords:
Disc bulging
Posterior stabilization
Lumbar spine
Soft tissue deformation
Motion preserving implants laser scanner

ABSTRACT

Background: The aims of motion preserving implants are to ensure sufficient stability to the spine, to release facet joints by also allowing a physiological loading to the intervertebral disc. The aim of this study was to assess disc load contribution by means of annular fiber strains and disc bulging of intact and stiffened segments. This was compared to the segments treated with various motion preserving implants.
Methods: A laser scanning device was used to obtain three-dimensional disc bulging and annular fiber strains of six lumbar intervertebral discs (L2–3). Specimens were loaded with 500 N or 7.5 Nm moments in a spine tester. Each specimen was treated with four different implants; DSS™, internal fixator, Coflex™, and TOPS™.
Findings: In axial compression, all implants performed in a similar way. In flexion, the Coflex decreased range of motion by 13%, whereas bulging and fiber strains were similar to intact. The DSS stabilized segments by 54% compared to intact. TOPS showed a slight decrease in fiber strains (5%) with a range of motion similar to intact. The rigid fixator allowed strains up to 2%. In lateral bending, TOPS yielded range of motion values similar to intact, but maximum fiber strains doubled from 6.5% (intact) to 13.8%. Coflex showed range of motion, bulging and strain values similar to intact. The DSS and the rigid fixator reduced these values. The implants produced only minor changes in axial rotation.
Interpretation: This study introduces an in vitro method, which was employed to evaluate spinal implants other than standard biomechanical methods. We could demonstrate that dynamic stabilization methods are able to keep fiber strains and disc bulging in a physiological range.

1. Introduction

Rigid fixation of lumbar spinal segments was considered to be the “golden standard” in the treatment of intervertebral disc (IVD) degeneration. Motion preserving implants were introduced as a spinal treatment alternative to address the potential disadvantageous effects on the adjacent segments. These implants should keep the segment flexible, but should also stabilize the segment, if clinically indicated. Posterior motion preserving implants were developed to retain the IVD, maintaining as much of the anatomical structures as possible. There is a large variety of posterior motion preserving implants, like the Dynesys (Zimmer, Minneapolis MN, USA)(Stoll et al., 2002), the facet replacement TOPS (Impliant Ltd, Ramat Poleg, Israel) (Wilke et al., 2006a, 2006b) or X-Stop (St. Francis Medical Technologies Inc., Alameda CA, USA) (Christie et al., 2005). The aims of motion preserving implants are to limit or guide spinal motion, to release the facet joints and to still allow a physiological loading to the IVD. This could reduce the higher stress in the adjacent segments instead of stiffening the segments.

The quality of mechanical loading (Urban and McMullin, 1988). Limitation or a strong reduction of IVD motion negatively influences the biological environment of the discs. This can lead to a transformation of the cell matrix resulting in an acceleration of disc degeneration (Lotz et al., 1998). A dynamic stabilization of the spine allows for an active nutrition transport and can also stimulate cell growth. It is assumed that under physiological conditions disc regeneration or at least a retardation of the disc degeneration can be achieved (Hutton et al., 1999; Neidlinger-Wilke et al., 2004; Rannou et al., 2003). To evaluate whether the load transmission through the disc has changed from the physiological condition, it is required to study other measurement parameters. To conduct three-dimensional disc bulging and disc surface strains would be an interesting alternative to standard biomechanical testing. In the past, ultimate tensile strains were determined from the annulus fibrosus(Ebara et al., 1996; Galante, 1967; Holzapfel et al., 2005; Iatridis et al., 2005; Shah et al., 1978). However, in most studies the disc is sectioned in order to extract samples from the annulus. To study the interaction of IVD loading and its annulus strain it is required to obtain the internal IVD strain distribution (Costi et al., 2007; Seroussi et al., 1989) or to obtain the strain at

* Corresponding author at: Institute of Orthopaedic Research and Biomechanics, Center of Musculoskeletal Research Ulm (ZMFU), University Hospital Ulm, Helmholtzstr. 14, 89081 Ulm, Germany.
E-mail address: hans-joachim.wilke@uni-ulm.de (H.-J. Wilke).

0268-0033/$ – see front matter
doi:10.1016/j.clinbiomech.2011.09.004

the outer annulus surface, if the IVD should be measured without any damages. Still, little is known about the outer IVD surface strain distribution of the physiological (intact) condition. This problem especially accounts for the aim of studying how posterior IVD preserving implants might affect the outer annulus strain distribution.

Local strains along the disc surface could provide a measure for the existing load condition: for the intact condition or with implants in place. The aim of this study was investigate how different treatment methods influence the biomechanics of intervertebral discs. For this purpose, we studied disc deformations in terms of strains and bulging in combination with RoM with four different implant designs. Our hypothesis was that an implant would not increase disc bulging and/or fiber associated strains compared the intact situation.

2. Methods

2.1. Disc contour scanner

A three-dimensional laser scanning device was used (Heuer et al., 2007) and placed inside a spine tester (Wilke et al., 1994) (Fig. 1). The setup consists of a rotation arm holding a laser profile sensor (scanControl 2800–25, MicroEpsilon, Ortenburg, Germany) (Heuer et al., 2008a, 2008b, 2008c). This sensor rotates about the specimen while the specimen is loaded in the spine tester. The laser scanner provides an accuracy of 10 μm in radius, 25 μm in height and 0.04° in circumference. It is capable of obtaining 1024 points per profile. The maximal profile sampling rate is 1 kHz.

2.2. Specimen preparation

Six human lumbar spinal segments (L2-3) with a median age of 51 years (range: 38–59) were used in this experiment. Specimens with bony defects or with a disc degeneration degree more than one (Wilke et al., 2006a, 2006b) were excluded from this study ensuring similar conditions. Soft tissue of specimens was stripped off while preserving ligaments, facet capsules and the IVD. Before potting, specimens were held with a custom-made fixture, which allowed an IVD alignment of the specimens. Specimens were orientated so that the mid-horizontal IVD plane was parallel to the lower casting mold. Then, the cranial and the caudal end of the segments were embedded in polymethylmethacrylate.

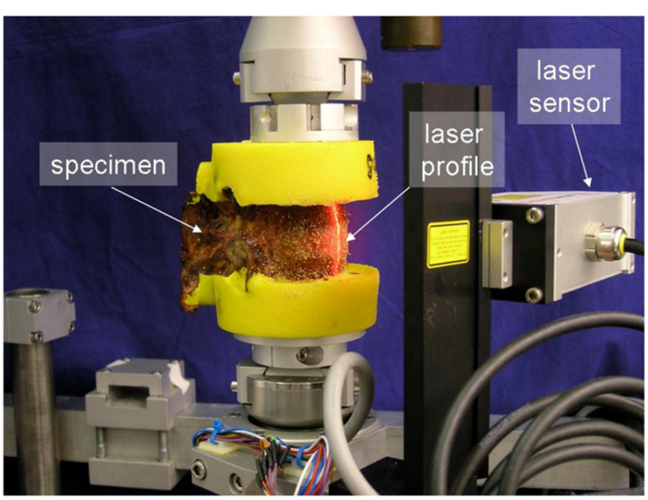

Fig. 1. Six L2–3 specimens were loaded in the spine tester with pure bending moments of 7.5 Nm. Surfaces of the specimens were obtained with a custom-built laser scanning system. This laser scanner rotated about the specimen while it acquired the spatial data within a single turn. Surface data were assessed for all loading directions including axial compression, flexion, extension, lateral bending and axial torque.

The endplates above and below the IVD of interest were marked using three steel pins. One was inserted anteriorly and the others were placed at both lateral sides. These pins were registered after the data processing to be able to distinguish the disc from the vertebrae. Subsequently, the specimen surface (vertebral bodies and the IVD) was coated with an artificial roughness fixed to the surface using an adhesive spray (Band-Aid, Johnson and Johnson Wound Ethicon, Germany). It can be assumed that this glue did not constrain the measurement surface. This surface roughness produced a randomized and stochastically distributed “salt-and-pepper” pattern to the disc surface, which was required to detect surface deformation using image processing algorithms (Sutton et al., 2000).

2.3. Experimental protocol

The laser scanner was mounted to the spine tester frame before the experiment. Then, the caudal end of the segment (L3) was affixed to the laser scanner base. The cranial end of L2 was fixed to the gimbal system of the spine tester. Prior to the experiments, specimens were exposed for 15 min to 500 N axial compression to reduce the water content of specimens (Adams et al., 1988). A base-line scan of the three-dimensional IVD contour was obtained from the unloaded specimens with 512 points per profile in height and 720 points along the circumference (Fig. 1). After the initial scan, an axial compression of 500 N or pure unconstrained bending moments of 7.5 Nm were applied to the specimens. Specimens were exposed to flexion, extension, lateral bending and axial rotation movements. Maximal deflections were evaluated from the RoM and neutral zone assessment. Subsequently, specimens were brought into the positions recorded at 7.5 Nm and held in this position. Surface scans were performed in this position. A scan required 4 s and it can be assumed that the contours did not change due to the viscoelastic properties of the IVD (Heuer et al., 2007). After the measurements on the intact (non-treated) segments, four different implants were employed and evaluated by means of RoM, disc bulging and annular fiber strains.

2.4. Sequence of implanting

The Dynamic Stabilization System (DSS™, Paradigm Spine, Wurmlingen, Germany) has the task to support a destabilized spine from the posterior site, but not to fuse. This system consists of two spring-a-like column elements, which are internally limited to a maximal displacement of approximately 2 mm in each direction (Fig. 2). The implant can be flexible aligned in different ways on the pedicle screws. The implants are adjustable and available in different sizes to ideally bridge the posterior elements. Implantation was performed by inserting pedicle screws with 5 mm diameter. Subsequently, the implant was mounted to these pedicle screws.

The next implant was an internal rigid fixator (Int.Fix.). This implant was utilized in this study to provide a second control reference for the evaluation, because it exhibits a non-dynamic implant. Pedicle screws of the DSS™ implant were taken off from specimens. Subsequently, pedicle screws with a diameter of 6.5 mm (Impliant Ltd, Ramat Poleg, Israel) were placed in the predrilled holes. Rigid bars (ART™, AMT, Nonnweiler, Germany) were connected to the screws fixing the spine.

An interspinous implant, the Coflex™ (Paradigm Spine, Wurmlingen, Germany), was used in the next step. For this purpose, the interspinous and supraspinous ligaments were removed. Subsequently, the Coflex™ was inserted in-between the spinous processes measuring the correct implant size. Implants were not crimped, because they should not limit flexion movements. However, the task of this implant is to limit extension movements, providing a posterior decompression.

In the last step, a bilateral laminectomy, including facetectomy of the lower facet joints, of the upper vertebra (L2) was performed prior to implantation of the TOPS™ (Impliant Ltd, Ramat Poleg, Israel)

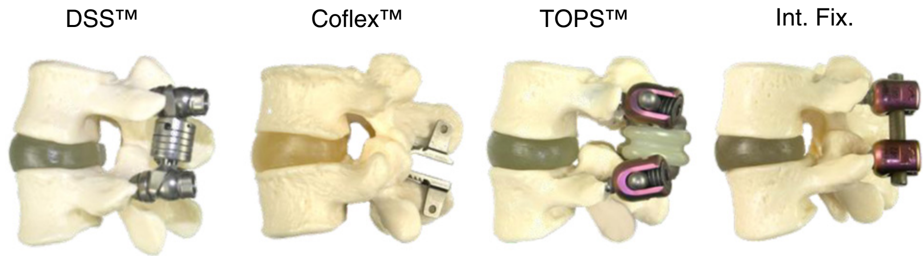

Fig. 2. Three different posterior motion preserving implants were evaluated and compared to the non-treated condition. Furthermore, an internal fixator was utilized to mimic a rigidly fixed situation. Following implants were considered: DSS™, interspinous implant Coflex™, a total facet joint replacement (TOPS™) and an internal fixator (Int. Fix.).

implant. Then, the TOPS™ implant was mounted on the pedicle screws, which were left in place from the internal rigid fixator. This implant is used to replace the facet joints and to provide physiological motion close to that of the natural condition.

2.5. Data Evaluation

Surface scan data were assigned to a gray-scale-like pattern, which allowed for a determination of displacement vectors between surface data obtained from specimens in a loaded and unloaded situation. Surface scan data were investigated using image processing algorithms (Heuer et al., 2008a, 2008b, 2008c). These displacement vectors were then taken as starting condition for the surface strains computation using the ANSYS V11.0 package (Swanson Analysis, Houston, PA, USA). Nodes (IVD surface points) together with the element table were imported to ANSYS. Displacement data from in vitro measurements were taken as boundary conditions for each node of the four-node shell elements. These included the surface strains components along the axial, circumferential and shear direction. Based on this it is possible to determine a strain component in another direction, like fiber orientated strains. Fiber strains were evaluated along the annulus fiber directions, inferring from fiber associated strain. The fiber angles were obtained from a study by Holzapfel et al.(2005). Furthermore, fiber angles were distinguished between clockwise (CW) and counterclockwise (CCW) orientation. A clockwise orientation means that the fibers go from the upper endplate in a clockwise direction into the lower endplate of the IVD.

Disc bulging was determined in the same way. The displacement vectors also contained the information of the upper vertebra translation, which was determined using the ANSYS. Details of bulging evaluation were reported early in detail (Heuer et al., 2008a, 2008b, 2008c). This translation was subtracted from the deformation map and we obtained disc bulging of the entire IVD surface. All data were summarized using the median function.

Due to the limited sample size, RoM data were assumed to be non-normally distributed, therefore, a general nonparametric test for more than two conditions of one specimen's group, the Friedmann-test, was used to proof for tendencies of significance. If the Friedmann-test resulted in a $p<0.05$ then a Wilcoxon's *U*-test (signed rank test) was used to show statistical significant differences between steps. In all tests, p-values with less than 0.05 were considered to show a significant difference.

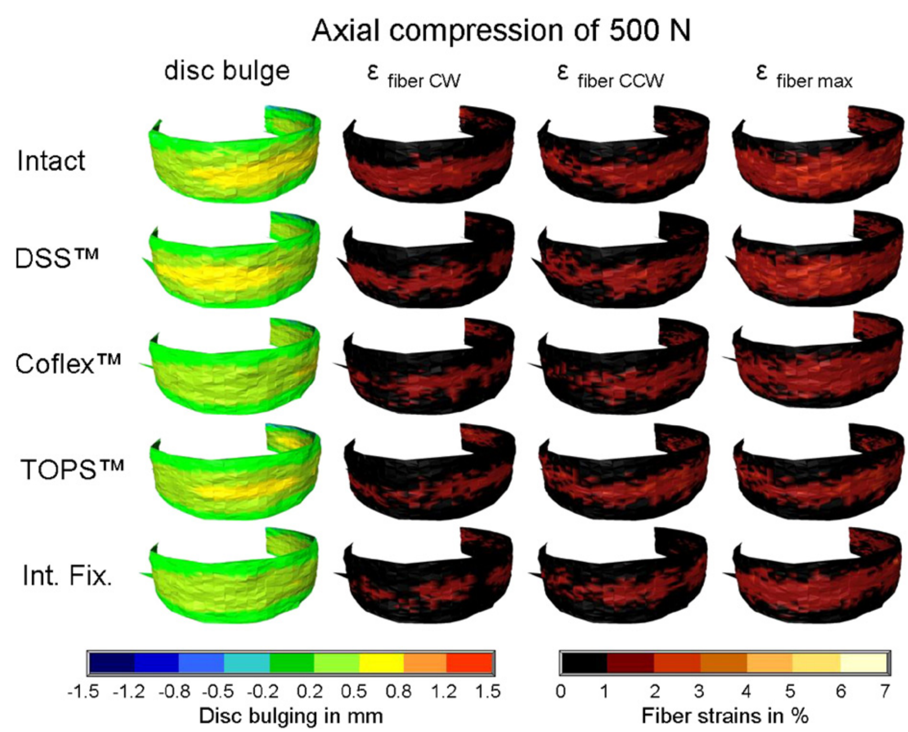

Fig. 3. Oblique front view at four different implants and the intact condition were exposed to an axial compression of 500 N. These specimen conditions were evaluated for disc bulging and strains of clockwise (ε_{CW}) and counterclockwise (ε_{CCW}) orientated annular fibers. Both fiber directions were summarized in the (ε_{max}) illustration. This parameter considered both fiber directions, whereas the maximum value of CW or CCW was assigned to the (max). All data contain the median of all specimens.

Table 1
Maximum tensile strains of the collagen fibers in the six specimens. Summarized are the load directions and inserted implants.

Implants	Load direction				
	Axial compression	Flexion	Extension	Lateral bending	Axial rotation
Intact	2.7%	7.2%	4.0%	6.5%	3.1%
DSS™	3.0%	2.4%	1.1%	3.1%	2.1%
Coflex™	3.9%	10.5%	1.6%	6.8%	2.7%
TOPS™	3.5%	5.0%	5.3%	13.8%	3.4%
Int. Fix.	3.1%	2.0%	1.2%	1.3%	1.9%

3. Results

For axial compression, it was found that all stabilization systems performed very similarly with an averaged maximum fiber strain of 3.2% (Fig. 3 and Table 1). The Coflex™ system slightly limited the disc from bulging at the lateral and posterolateral site. This could be due to the decompression effect at the posterior elements by the implant.

Flexion produced the largest disc bulging in the non-treated situation (Fig. 4). Maximum disc bulging was found at the anterior region with an outward bulging of 1.6 mm. Fiber strains of a maximum of 7.2% were obtained at the anterior region, as well. Both directions (CW and CCW) showed a symmetrical response of the active fibers. The Coflex™ system performed a similar range of motion in flexion (12% reduction) and also resulted in a comparable disc bulging as for intact condition (Fig. 5). Fiber strain distribution seemed to be similar to intact, but the maximum fiber strain value was greater than 10%. The DSS™ implant stabilized the specimens with 54% compared to the RoM of the non-treated condition. This decreased the disc bulging and fiber strains to 2.4%, accordingly. The same effect was seen for the internal fixator. Fiber strains were as low as 2%. The facet joint replacement implant (TOPS™) led to a smaller bulging of the IVD compared to the intact condition. This also slightly reduced the fiber strains (5%) of the frontal and lateral IVDs.

In extension a maximum inward disc bulging of 0.7 mm was recorded for the specimens without implants (Fig. 6). This was accompanied by a maximum fiber strain of 4% in the lateral and posterolateral region. The fibers of the frontal IVD remained unloaded. The non-treated specimens showed a RoM of 3.4°. A RoM of 3.5° was obtained for the specimens when the TOPS™ system was in place. This implant did not essentially increase the fiber strains (5.3%) compared to the non-treated condition. The Coflex™, DSS™ and internal fixator were more effective with regard to stabilization resulting in an average decrease in disc bulging to 0.47 mm. Fiber strains with less than 2% were negligible for the DSS™, Coflex™ and the internal fixator.

Lateral bending caused large fiber strains assessed in this setup. Fibers were mostly loaded in the direction of bending. Fiber strains up to 6.5% and a maximum disc bulging of 1.1 mm were recorded for non-treated specimens (Fig. 7). Insertion of the internal fixator decreased disc bulging and fiber strains to 1.3%. This implant almost released the IVD from the applied load. The DSS™ system stabilized the segments by 45% regarding the RoM. This was also seen with regard to disc bulging and fiber strains (3.1%). The Coflex™ performed similar compared to the non-treated condition with 6.8% fiber strain. However, the TOPS™ implant increased disc bulging by a value of 0.3 mm also increasing fiber strains up to 13.8%.

Axial rotation was indicated by that the fibers in the CW direction were tensioned up to 3.1% whereas the CCW orientated fibers remained non-tensioned (Fig. 8). Disc bulging data showed an inward bulging at the right front IVD location. This bulging was aligned in an oblique direction between the endplates. The internal fixator stiffened the RoM, which resulted in a decrease in the fiber strains and disc bulging. The Coflex™ performed similar compared to the non-treated segments. The segments with the DSS™ implant showed a decrease in disc bulging compared to the intact condition,

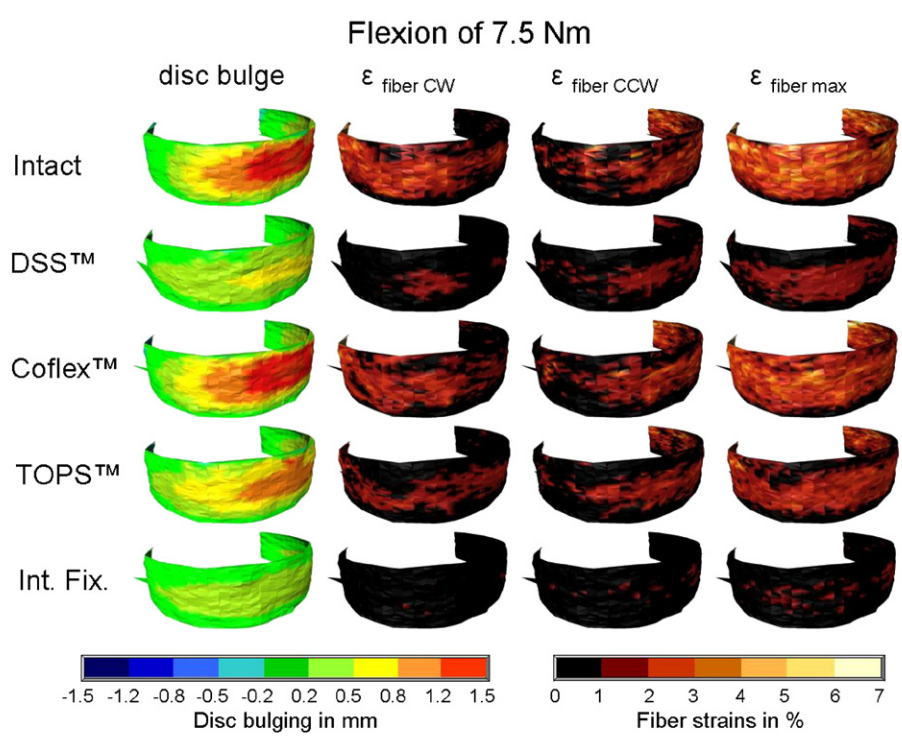

Fig. 4. Oblique front view at four different implants and the intact condition were analyzed when the specimens were bended in flexion. This figure shows disc bulging and fiber strains (ε) in clockwise (CW), counterclockwise (CCW) and both (max) directions.

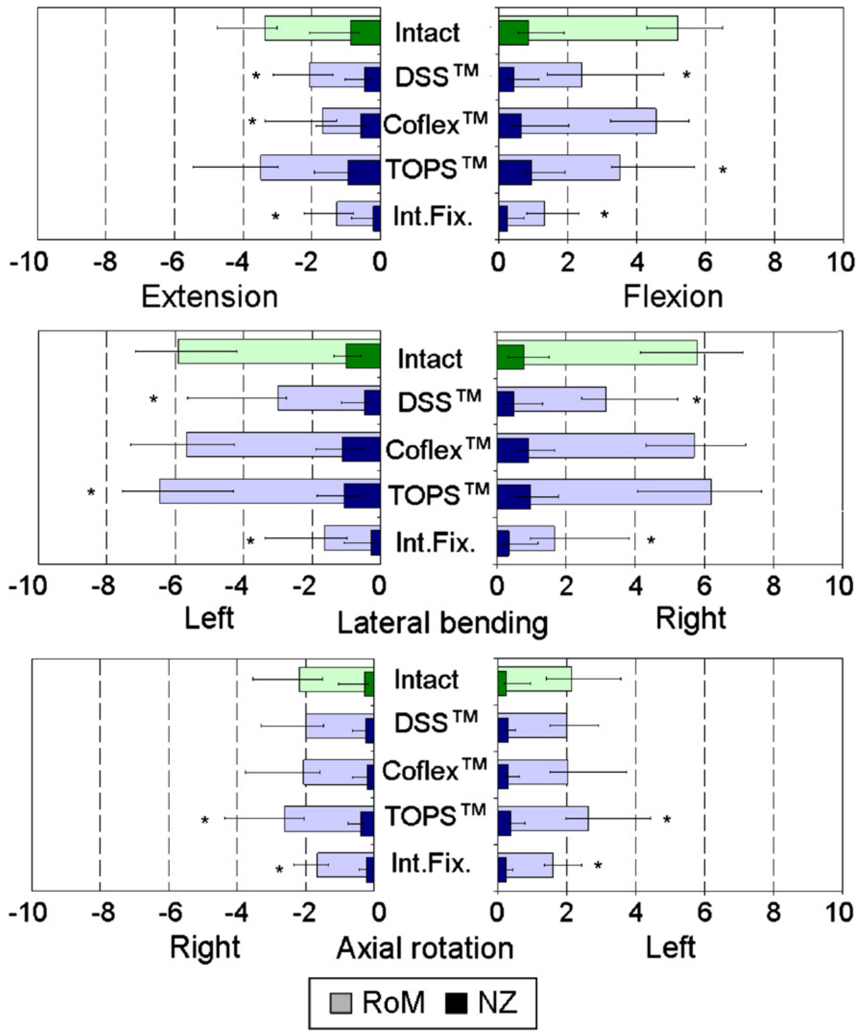

Fig. 5. Range of motion (RoM) and neutral zone (NZ) in degrees. Tested were the six specimens in lateral bending, flexion, extension and axial rotation. The four implants were evaluated by means of the RoM and NZ data. (*) significantly different from the intact condition indicated by the Wilcoxon signed rank test.

but RoM was comparable to the non-treated segments with 7% RoM reduction. However, fiber strains were located in opposite regions of the disc for the DSS™ implant. They changed from the left to the right side of the disc during axial rotation. The TOPS™ implant had a slightly larger RoM compared to the non-treated condition. This was also accompanied by slightly higher fiber strains and disc bulging.

4. Discussion

The aims of motion preserving implants are to provide stability to the segment, but also preserving the IVD. This study could demonstrate that various implant concepts lead to different strain and bulge distributions on the disc. These results were conducted from a new measurement method, which was used to obtain three-dimensional surface scans yielding annular fiber strains and disc bulging. Four different implants designs were tested, each with a different indication, but with the aim of preserving the disc and maintaining a certain degree of spinal motion. The hypothesis that an implant does not increase disc bulging or fiber associated strains compared to the intact situation has not been confirmed.

The intact condition served as control, which was assumed to exhibit the physiological condition. The second control was given by the rigid internal fixator. Results of the flexibility assessment showed that the rigid fixator strongly stabilized the segments compared to the non-treated situation. This was also seen in the surface strain data. The testing of the rigid fixator was considered to provide the second reference for the comparison of the motion preserving implants. The motion preserving implants performed in-between the given two extreme conditions (intact and rigid). It was also shown that the internal fixator could limit the RoM and caused a limitation in disc bulging and fiber strains for the bending and torsional moments. Interestingly, it was demonstrated that this rigid stabilization system did not prevent the disc from axial loading since all implants performed similar in axial compression.

The DSS™ is a new implant design; therefore no comparison to former studies can be made. Regarding the performance of this device, some motion was still allowed by the implant construct. For bending loads, fiber strains were seen in the range of about half of the intact segments. However, it was more flexible compared to the rigid fixator, but stiffer than the Coflex™ and the TOPS™ implant.

The Coflex™ implant has the function to limit the movements in extension in order to decompress the posterior elements. RoM in flexion was reduced to a minor degree (12%), while extension was limited by 50% of the motion. This relation of RoM reduction was in good agreement to previous findings(Tsai et al., 2006). Else, the implant performed with regard to disc bulging and fiber strains comparable to the non-treated condition. The implant slightly reduced the RoM in flexion. In contrast, it yielded a slight increase in the fiber strains.

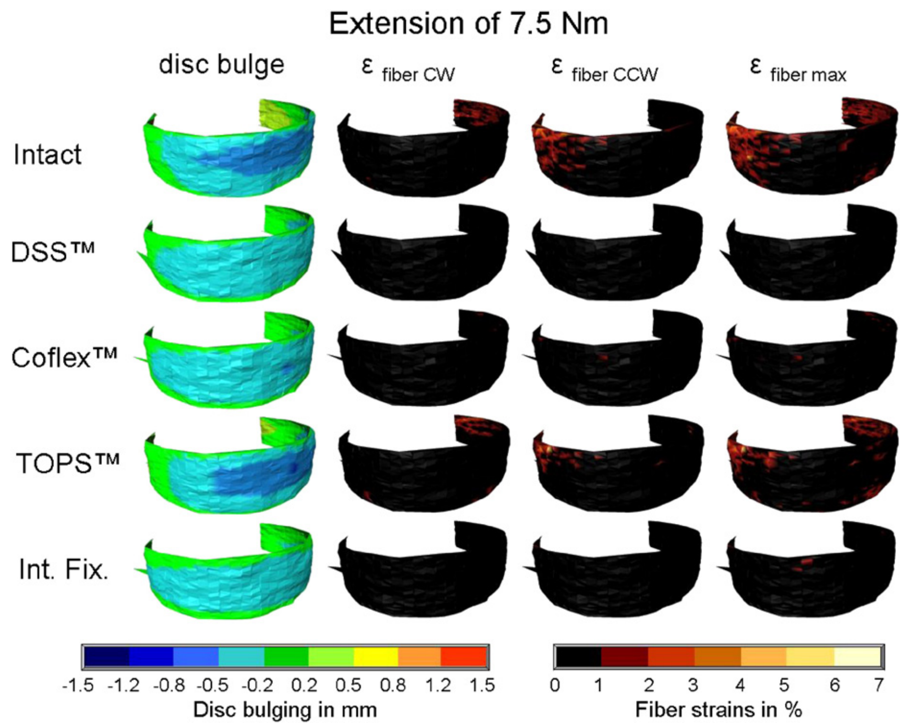

Fig. 6. Four different implants and the intact condition were analyzed when the specimens were bended in extension. This figure shows an oblique front view of disc bulging and fiber strains (ε) in clockwise (CW), counterclockwise (CCW) and both (max) directions.

The TOPS™ implant was designed to replace the posterior elements including the facet joints of a lumbar spinal segment, but to preserving the IVD at the same time. RoM assessment showed that this implant was capable to restore the RoM in axial rotation, lateral bending and to about 82% of flexion/extension movements. This finding was comparable to reported 85%(Wilke et al., 2006a, 2006b). However, in lateral bending a slight increase in the RoM was obtained. This slight increase, however, induced almost double of the maximum fiber strains found

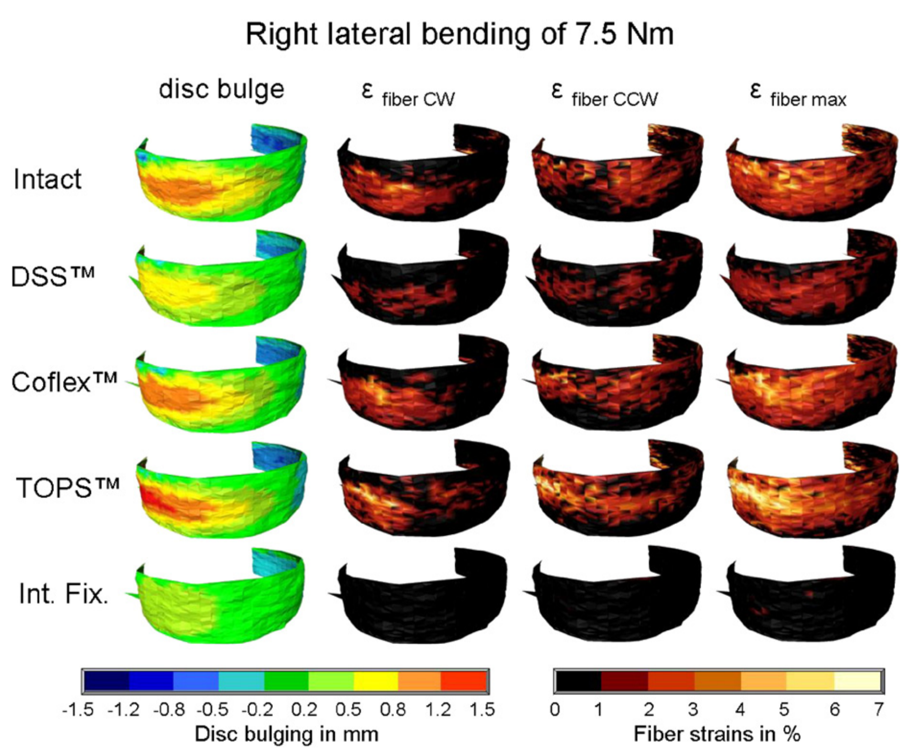

Fig. 7. Right lateral bending was applied to specimens in a non-treated condition and after the DSS™, Coflex™, internal fixator (Int. Fix.) and the TOPS™ were inserted. These conditions were evaluated by means of disc bulging, clockwise (ε_{CW}), counterclockwise (ε_{CCW}) and the (ε_{max}) fiber strains. An oblique front view is shown.

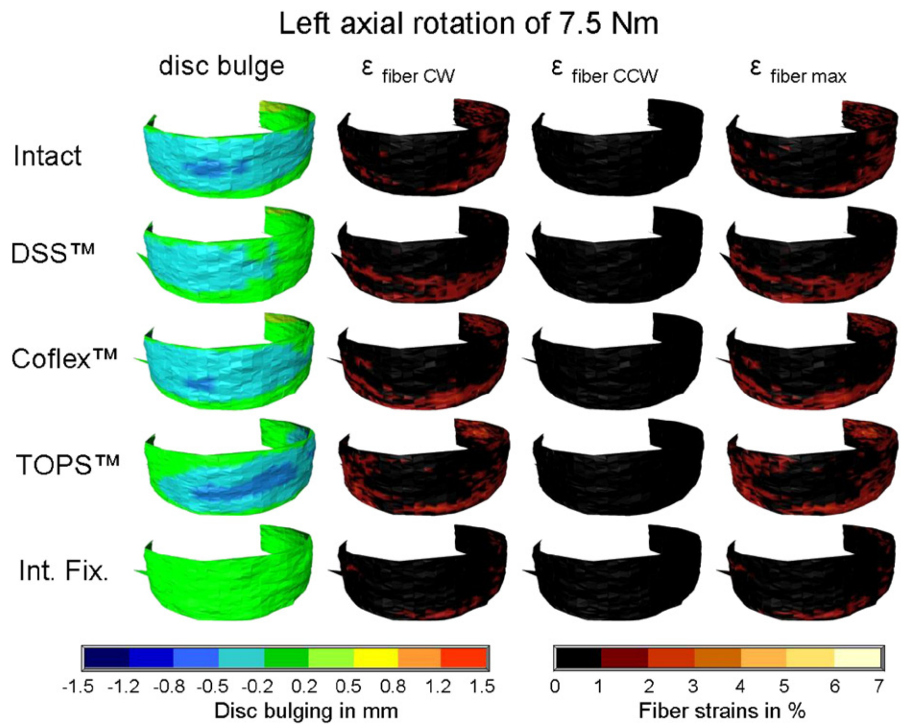

Fig. 8. Four different implants and the intact condition were analyzed when the specimens were exposed to torsional moments producing left axial rotation. This figure delineates disc bulging, clockwise (CW), counterclockwise (CCW) and the (max) fiber strains (ε).

for the intact condition. In contrast to the potential of the implant to restore the biomechanics back to intact values, it has to be mentioned that many functional bony structures have to be sacrificed during the implantation. It preserves the IVD, but requires the removal of the vertebral arches, facet joints and attached posterior ligaments.

The trend in the regularly biomechanical evaluation of spinal implants is to measure both the RoM and intradiscal pressure(Schmoelz et al., 2003; Wilke et al., 1998). The RoM can provide a general description of how the implant stabilizes the spinal segment. The intradiscal pressure was often considered to yield the load contribution of the disc. This is a rough estimation, because the intradiscal pressure does not always indicate a specific load situation in the disc. For example, a complex load pattern can cause high stresses to the disc compared to a pure axial compression, which would also reflect the same intradiscal pressure(Schmidt et al., 2007). Therefore, the fiber strains of the annulus surface together with the disc bulging might give a better description for the load contribution of the disc.

This new method of measuring the IVD surface strain provides the potential of evaluating the load distribution of the outer annulus. This method is very sensitive against and fast deployable during the regularly RoM assessment. It might indicate better the load contribution of the IVD compared to measuring the intradiscal pressure. Furthermore, the distribution of the load can be assessed. However, this method is limited to the annulus surface and needs a free sight to the object. Additional or complementary data can be provided by utilizing a finite element model computing the missing part of the surface strains. This technique of predicting the non-accessible posterior and posterolateral part of the IVD was reported for three-dimensional disc displacements (Heuer et al., 2008a, 2008b, 2008c).

Spinal motion produced by pure unconstrained moments without preload may not be necessarily physiological, but it provides reproducibility (Wilke et al., 1998). Another limitation is the testing sequence. A different sequence of implanting could potentially lead to different results. However, the sequence was predetermined by application requirements of the utilized implants in this study.

Intervertebral disc degeneration could affect the strain pattern of the discs, especially when osteophytes were formed. In Addition, the implantation of the motion preserving stabilization devices could differently affect the motion respond because of degenerative changes of the segments. Therefore, this study considered only none or mildly degenerated specimens for the measurements to exclude this error source and to feature the same conditions.

In conclusion, it can be stated that motion preserving implants are capable to at least partially keep the natural fiber strain and bulging distribution of the IVDs. Furthermore, this was put into comparison to a rigid fixator, which stiffened the situation and the major part of the load was transferred through the fixation rods. This produced smallest fiber strains. Assuming that the intact situation is presenting the ideal condition, the Coflex™ and TOPS™ implant lead to physiological conditions regarding the fiber strains and disc bulging. The DSS™ system maintained nearly half of the intact motion, but it was more flexible than the rigid fixation system.

Acknowledgments

This study was financially supported by the German Research Foundation (Wi-1356/10-1). Implants were provided without costs by the companies (ParadigmSpine, AMT and Impliant). No additional funding was received.

References

Adams, M.A., Dolan, P., Hutton, W.C., 1988. The lumbar spine in backward bending. Spine 13 (9), 1019–1026.
Christie, S.D., Song, J.K., Fessler, R.G., 2005. Dynamic interspinous process technology. Spine 30 (16 Suppl), S73–S78.
Costi, J.J., Stokes, I.A., Gardner-Morse, M., Laible, J.P., Scoffone, H.M., Iatridis, J.C., 2007. Direct measurement of intervertebral disc maximum shear strain in six degrees of freedom: Motions that place disc tissue at risk of injury. J. Biomech. 40 (11), 2457–2466.

Ebara, S., Iatridis, J.C., Setton, L.A., Foster, R.J., Mow, V.C., Weidenbaum, M., 1996. Tensile properties of nondegenerate human lumbar anulus fibrosus. Spine 21 (4), 452–461.

Galante, J.O., 1967. Tensile properties of the human lumbar annulus fibrosus. Acta Orthop. Scand. Suppl. 100, 101–191.

Heuer, F., Schmitt, H., Schmidt, H., Claes, L., Wilke, H.J., 2007. Creep associated changes in intervertebral disc bulging obtained with a laser scanning device. Clin. Biomech. 22 (7), 737–744.

Heuer, F., Schmidt, H., Claes, L., Wilke, H.J., 2008a. A new laser scanning technique for imaging intervertebral disc displacement and its application to modeling nucleotomy. Clin. Biomech. 23 (3), 260–269.

Heuer, F., Schmidt, H., Wilke, H.J., 2008b. The relation between intervertebral disc bulging and annular fiber associated strains for simple and complex loading. J. Biomech. 41 (5), 1086–1094.

Heuer, F., Wolfram, U., Schmidt, H., Wilke, H.J., 2008c. A method to obtain surface strains of soft tissues using a laser scanning device. J. Biomech. 41 (11), 2402–2410.

Holzapfel, G.A., Schulze-Bauer, C.A., Feigl, G., Regitnig, P., 2005. Single lamellar mechanics of the human lumbar anulus fibrosus. Biomech. Model. Mechanobiol. 3 (3), 125–140.

Hutton, W.C., Elmer, W.A., Boden, S.D., Hyon, S., Toribatake, Y., Tomita, K., et al., 1999. The effect of hydrostatic pressure on intervertebral disc metabolism. Spine 24 (15), 1507–1515.

Iatridis, J.C., MaClean, J.J., Ryan, D.A., 2005. Mechanical damage to the intervertebral disc annulus fibrosus subjected to tensile loading. J. Biomech. 38 (3), 557–565.

Lotz, J.C., Colliou, O.K., Chin, J.R., Duncan, N.A., Liebenberg, E., 1998. Compression-induced degeneration of the intervertebral disc: an in vivo mouse model and finite-element study. Spine 23 (23), 2493–2506.

Neidlinger-Wilke, C., Würtz, K., Schmidt, C., Blessing, H., Börm, W., Arand, M., et al., 2004. Effects of mechanical forces on intervertebral disc cells from annulus and nucleus of human and bovine discs. Combined Meeting of Leading Scientifig Spine Societies, Porto.

Rannou, F., Richette, P., Benallaoua, M., Francois, M., Genries, V., Korwin-Zmijowska, C., et al., 2003. Cyclic tensile stretch modulates proteoglycan production by intervertebral disc annulus fibrosus cells through production of nitrite oxide. J. Cell. Biochem. 90 (1), 148–157.

Schmidt, H., Kettler, A., Heuer, F., Simon, U., Claes, L., Wilke, H.J., 2007. Intradiscal pressure, shear strain, and fiber strain in the intervertebral disc under combined loading. Spine 32 (7), 748–755.

Schmoelz, W., Huber, J.F., Nydegger, T., Claes, L., Wilke, H.J., 2003. Dynamic stabilization of the lumbar spine and its effects on adjacent segments: an in vitro experiment. J. Spinal Disord. Tech. 16 (4), 418–423.

Seroussi, R.E., Krag, M.H., Muller, D.L., Pope, M.H., 1989. Internal deformations of intact and denucleated human lumbar discs subjected to compression, flexion, and extension loads. J. Orthop. Res. 7 (1), 122–131.

Shah, J.S., Hampson, W.G., Jayson, M.I., 1978. The distribution of surface strain in the cadaveric lumbar spine. J. Bone Joint Surg. (Br. Ed.) 60-B (2), 246–251.

Stoll, T.M., Dubois, G., Schwarzenbach, O., 2002. The dynamic neutralization system for the spine: a multi-center study of a novel non-fusion system. Eur. Spine J. 11 (Suppl 2), S170–S178.

Sutton, M.A., McNeill, S.R., Helm, J.D., Chao, Y.J., 2000. Photomechanics Advances in Two-Dimensional and Three-Dimensional Computer Vision. In: Rastogi, P.K. (Ed.), Photomechanics. : Topics in Applied Physics, 77. Springer-Verlag Berlin, Heidelberg, pp. 323–372.

Tsai, K.J., Murakami, H., Lowery, G.L., Hutton, W.C., 2006. A biomechanical evaluation of an interspinous device (Coflex) used to stabilize the lumbar spine. J. Surg. Orthop. Adv. 15 (3), 167–172.

Urban, J.P., McMullin, J.F., 1988. Swelling pressure of the lumbar intervertebral discs: influence of age, spinal level, composition, and degeneration. Spine 13 (2), 179–187.

Wilke, H.J., Claes, L., Schmitt, H., Wolf, S., 1994. A universal spine tester for in vitro experiments with muscle force simulation. Eur. Spine J. 3 (2), 91–97.

Wilke, H.J., Wenger, K., Claes, L., 1998. Testing criteria for spinal implants: recommendations for the standardization of in vitro stability testing of spinal implants. Eur. Spine J. 7 (2), 148–154.

Wilke, H.J., Rohlmann, F., Neidlinger-Wilke, C., Werner, K., Claes, L., Kettler, A., 2006a. Validity and interobserver agreement of a new radiographic grading system for intervertebral disc degeneration: Part I. Lumbar spine. Eur. Spine J. 15 (6), 720–730.

Wilke, H.J., Schmidt, H., Werner, K., Schmolz, W., Drumm, J., 2006b. Biomechanical evaluation of a new total posterior-element replacement system. Spine 31 (24), 2790–2796 discussion 2797.